EUR 5047 e

COMMISSION OF THE EUROPEAN COMMUNITIES

THE INVERTED STATISTICAL CHOPPER FACILITY FOR ELASTIC AND INELASTIC NEUTRON SCATTERING EXPERIMENTS

by

W. KLEY and W. MATTHES

1974

Joint Nuclear Research Centre
Ispra Establishment - Italy

LEGAL NOTICE

This report is on sale at the addresses listed on cover page 4

at the price of B.Fr. 50 .

Commission of the
European Communities
D.G. XIII - C.I.D.
29, rue Aldringen
L u x e m b o u r g
January 1974

EUR 5047 e

THE INVERTED STATISTICAL CHOPPER FACILITY FOR ELASTIC AND INELASTIC NEUTRON SCATTERING EXPERIMENTS
by W. KLEY and W. MATTHES

Commission of the European Communities
Joint Nuclear Research Centre — Ispra Establishment (Italy)
Luxembourg, January 1974 — 36 Pages — 16 Figures — B.Fr. 50.—

In this paper it is shown that the inverted time of flight spectrometer (inverted statistical chopper) has a large accessibility in the K, ω-plane and that the energy resolution function and the intensity is rather constant over a large energy range. The inverted geometry is therefore very favourable to perform precision measurements of line width and line shape of local modes, high energy phonons and magnons. In principle a 4πBe–MgO window detector can be built for high intensity low background experiments. The role of the statistical chopper is primarily to reduce the continuous elastic and inelastic background.

EUR 5047 e

THE INVERTED STATISTICAL CHOPPER FACILITY FOR ELASTIC AND INELASTIC NEUTRON SCATTERING EXPERIMENTS
by W. KLEY and W. MATTHES

Commission of the European Communities
Joint Nuclear Research Centre — Ispra Establishment (Italy)
Luxembourg, January 1974 — 36 Pages — 16 Figures — B.F.r 50.—

In this paper it is shown that the inverted time of flight spectrometer (inverted statistical chopper) has a large accessibility in the K, ω-plane and that the energy resolution function and the intensity is rather constant over a large energy range. The inverted geometry is therefore very favourable to perform precision measurements of line width and line shape of local modes, high energy phonons and magnons. In principle a 4πEe–MgO window detector can be built for high intensity low background experiments. The role of the statistical chopper is primarily to reduce the continuous elastic and inelastic background.

EUR 5047 e

THE INVERTED STATISTICAL CHOPPER FACILITY FOR ELASTIC AND INELASTIC NEUTRON SCATTERING EXPERIMENTS
by W. KLEY and W. MATTHES

Commission of the European Communities
Joint Nuclear Research Centre — Ispra Establishment (Italy)
Luxembourg, January 1974 — 36 Pages — 16 Figures — B.Fr. 50.—

In this paper it is shown that the inverted time of flight spectrometer (inverted statistical chopper) has a large accessibility in the K, ω-plane and that the energy resolution function and the intensity is rather constant over a large energy range. The inverted geometry is therefore very favourable to perform precision measurements of line width and line shape of local modes, high energy phonons and magnons. In principle a 4πBe–MgO window detector can be built for high intensity low background experiments. The role of the statistical chopper is primarily to reduce the continuous elastic and inelastic background.

All the results concerning the merits or advantages of a conventional statistical chopper compared to a common time of flight spectrometer are as valid for the inverted spectrometer.

An inverted statistical chopper facility is a useful and interesting spectrometer for high energy transfer measurements as well as for high resolution powder diffraction work.

All the results concerning the merits or advantages of a conventional statistical chopper compared to a common time of flight spectrometer are as valid for the inverted spectrometer.

An inverted statistical chopper facility is a useful and interesting spectrometer for high energy transfer measurements as well as for high resolution powder diffraction work.

All the results concerning the merits or advantages of a conventional statistical chopper compared to a common time of flight spectrometer are as valid for the inverted spectrometer.

An inverted statistical chopper facility is a useful and interesting spectrometer for high energy transfer measurements as well as for high resolution powder diffraction work.

EUR 5047 e

COMMISSION OF THE EUROPEAN COMMUNITIES

THE INVERTED STATISTICAL CHOPPER FACILITY FOR ELASTIC AND INELASTIC NEUTRON SCATTERING EXPERIMENTS

by

W. KLEY and W. MATTHES

1974

Joint Nuclear Research Centre
Ispra Establishment - Italy

ABSTRACT

In this paper it is shown that the inverted time of flight spectrometer (inverted statistical chopper) has a large accessibility in the K, ω-plane and that the energy resolution function and the intensity is rather constant over a large energy range. The inverted geometry is therefore very favourable to perform precision measurements of line width and line shape of local modes, high energy phonons and magnons. In principle a 4πBe–MgO window detector can be built for high intensity low background experiments. The role of the statistical chopper is primarily to reduce the continuous elastic and inelastic background.

All the results concerning the merits or advantages of a conventional statistical chopper compared to a common time of flight spectrometer are as valid for the inverted spectrometer.

An inverted statistical chopper facility is a useful and interesting spectrometer for high energy transfer measurements as well as for high resolution powder diffraction work.

KEYWORDS

TIME-OF-FLIGHT SPECTROMETERS
ENERGY RANGE
ENERGY RESOLUTION
PHONONS
MAGNONS
RESOLUTION
MEASURING INSTRUMENTS
PULSED NEUTRON TECHNIQUES
SCATTERING
COMPARATIVE EVALUATIONS

CONTENTS

I. Introduction

In 1968 the correlation technique has been introduced by a number of authors[1-6] for time of flight spectrometers at stationary reactors. The application of correlation techniques for pulsed neutron systems has been discussed also in the following years[7-14]. With the progress of the understanding of the correlation technique, the limitations of this method for stationary reactors appeared clearly. Weak lines cannot be measured in the presence of intense lines as is very often the case for coherent elastic and inelastic, and in particular, for incoherent elastic, quasi-elastic and inelastic scattering experiments. Also weak lines in the presence of large average intensities cannot be observed as obtained often in incoherent inelastic scattering experiments. These negative aspects do not enter so much in consideration for incoherent quasi-elastic scattering experiments, where the quasi-elastic line is dominant within a large $\vec{\kappa}$-range and of interest alone. The various theoretical analyses and also an experiment by Sköld[4] have demonstrated that the main advantage of the pseudo-statistical chopper appears in its application for experiments that have to be carried out with a large and uncorrelated background originated from the neutron beam impinging on the sample and from the room background of insufficiently shielded detectors. Certain problems in physics (diffraction, quasi-elastic scattering, high energy phonons, local modes, internal molecular modes, magnetic scattering, etc.) request information of the scattering law $S(\vec{\kappa},\omega)$ in a rather large range of $\vec{\kappa}$ and ω where

$$\vec{\kappa} = \vec{k}_i - \vec{k}_f$$

stands for the momentum- and

$$\hbar\omega = E_i - E_f = \frac{\hbar^2}{2m}(k_i^2 - k_f^2)$$

for the energy transfer in the scattering process. $\vec{k}_i$, $\vec{k}_f$ and E_i, E_f denote the initial and final neutron wave vector and the corresponding neutron energy.

This type of experiments requires high energy neutrons up to 1 eV and sometimes even higher. For a number of these experiments it is indicated to use a white neutron beam in order to cover the largest possible range in the $\vec{\kappa}, \omega$-plane. A white neutron beam, from a hot neutron source, is the most adequate one. For the energy definition of the neutrons of a white neutron beam, the time of flight method is the most appropriate one. The application of a statistical chopper in the white neutron beam that modulates neutrons with an energy below 1 eV, but not above 1 eV, is most useful, since a high duty cycle ($\approx 50\%$) can be used in the time of flight spectrometry and the continuous fast neutron background of the primary beam can be suppressed by the correlation technique as well as the room background.

In the following we are discussing the fields of application of the inverted statistical chopper and the theoretical aspects of the data analysis.

II. The Characteristic Parameters of a Conventional and Inverted Statistical Chopper Facility

II. 1 General Considerations Concerning the Intensity and Resolution of a Time of Flight Scattering Experiment Using a White Neutron Beam at a Hot Neutron Source

According to the notations of Fig. 1, the intensity of a scattering experiment at a pulsed neutron source is given by

$$(1) \quad J_{Detector} = \int \frac{1}{4\pi} \phi(E_i, \Omega_i, t) dE_i \cdot d\Omega_i \cdot dt \cdot \nu \cdot f_i F_T \cdot N \cdot d \cdot \frac{d^2\sigma}{d\Omega_f dE_f}(E_i, \Omega_i, E_f, \Omega_f) \cdot d\Omega_f \cdot dE_f \cdot f_f \cdot \varepsilon(E_f) \quad [n/sec]$$

where

$\phi(E_i, \Omega_i, t)$ is the flux per unit energy and per unit solid angle at the surface of the neutron source at time t

dE_i is the energy spread of the neutrons with energy E_i at the target

$d\Omega_i$ is the solid angle expanded by an area element dF_i of the neutron source area F_s. ($d\Omega_i = dF_i / \ell_i^2$ where ℓ_i is the distance source-target)

dt the time integration differential

t the time variable

ν the neutron source pulse frequency

f_i is a factor taking into account the intensity loss in the apparatus between the neutron source and the target

F_T is the effective target area (= neutron beam cross section)

N is the atom density of the target material

d is the effective target thickness

$$\frac{d^2}{d\Omega_f dE_f}(E_i, \Omega_i, E_f, \Omega_f) = \frac{\sigma_s}{4\pi} \cdot \frac{k_f}{k_i} \cdot S(\vec{K}, \omega)$$

is the differential scattering cross section

$\vec{k}_i$, $\vec{k}_f$ are the initial and final neutron momenta

$\vec{K} = \vec{k}_i - \vec{k}_f$ is the momentum transfer of the neutron on the target in the scattering process

$\hbar\omega = E_i - E_f$ is the energy transfer of the neutron on the target in the scattering process

$d\Omega_i$ is the solid angle element expanded by an area element dF_f of the neutron detector area F_D ($d\Omega_f = dF_f/\ell_f^2$, where ℓ_f is the distance target-detector)

dE_f is the energy spread of the neutrons with energy E_f at the detector

$\varepsilon(E_f)$ is the neutron detector efficiency

f_f is a factor taking into account the intensity loss in the apparatus between the target and the detector

If neutrons are scattered coherently from a single crystal, the elastic as well as the inelastic scattering cross section is given in terms of δ-fuctions and the integration [equation (1)] has to be carried out (integrated intensity). For all incoherent experiments the cross section is a rather smooth function of $|\vec{K}|$ and ω and therefore equation (1) can be written according to Maier-Leibnitz[15] in a more simplified manner. Assuming furthermore a continuous neutron source, the intensity of neutron scattering experiments using time of flight (T. O. F.)-techniques and conventional crystal spectrometry as outlined in Fig. 2, can be calculated by

$$(2) \quad J_{Detector} = \frac{1}{4\pi}\phi(E_i, \Omega_i) \cdot \Delta E_i \cdot \Delta\Omega_i \cdot \Delta t \cdot \nu \cdot f_i \cdot F_T \cdot N \cdot d \cdot \frac{d^2\sigma}{d\Omega_f dE_f} \cdot \Delta\Omega_f \cdot \Delta E_f \cdot f_f \cdot \varepsilon(E_f) \quad [n/sec] \ .$$

According to Fig. 3

$$(3) \quad \Delta\Omega_i = \frac{F_s}{\ell_i^2} = \frac{\Delta k_i^{(x)} \cdot \Delta k_i^{(y)}}{k_i^2}$$

$$(4) \quad \Delta\Omega_f = F_D / \ell_f^2 = \frac{\Delta k_f^{(x)} \cdot \Delta k_f^{(y)}}{k_f^2}$$

$$(5) \quad \frac{\Delta E_i}{E_i} = 2 \frac{\Delta k_i^{(z)}}{k_i} \quad ; \quad \frac{\Delta E_f}{E_f} = 2 \frac{\Delta k_f^{(z)}}{k_f}$$

$$(6) \quad \Delta E_i = \frac{\hbar^2}{2m} k_i . \Delta k_i^{(z)} \quad ; \quad \Delta E_f = \frac{\hbar^2}{2m} . k_f . \Delta k_f^{(z)}$$

$$(7) \quad \Delta V_i = \Delta k_i^{(x)} . \Delta k_i^{(y)} . \Delta k_i^{(z)} . \hbar^3$$

$$(8) \quad \Delta V_f = \Delta k_f^{(x)} . \Delta k_f^{(y)} . \Delta k_f^{(z)} . \hbar^3$$

and since for a scalar flux

$$(9) \quad \phi(E_i, \Omega_i) = \phi_{total} . \varepsilon^{-E_i/E_T} . \frac{E_i}{E_T} . \frac{\Delta E_i}{E_T}$$

and furthermore

$$(10) \quad E_T = k_B . T = \frac{\hbar^2}{2m} . k_T^2 \quad ; \quad E_i = \frac{\hbar^2}{2m} . k_i^2 \quad ; \quad E_f = \frac{\hbar^2}{2m} . k_f^2$$

$$(11) \quad \vec{\kappa} = \vec{k_i} - \vec{k_f} \quad ; \quad \hbar\omega = E_i - E_f = \frac{\hbar^2}{2m} (k_i^2 - k_f^2)$$

we can rewrite equation (2)

$$(12) \quad J_{Detector} = A(T) . f_i . F_T . N . d . \sigma_s . S(\vec{\kappa}, \omega) . f_f . \Delta V_i . \Delta V_f . \varepsilon(E_f)$$

$$(13)\quad A(T) = \frac{\Phi_{\text{total}}}{8\pi^2 m\hbar^4} \cdot \frac{e^{-k_i^2/k_T^2}}{k_T^4} = \frac{1}{4\pi m^2}\rho(T)$$

and

$$(14)\quad \rho(T) = \frac{\Delta n}{\Delta V_i} = \frac{\Phi_{\text{total}}}{2\pi} \cdot \frac{m}{\hbar^4} \cdot \frac{e^{-k_i^2/k_T^2}}{k_T^4} \cdot$$

$\rho(T)$ stands for the neutron density in momentum space. The intensity at the target and the detector is therefore proportional to

$$(15)\quad J_{\text{Target}} \approx \frac{e^{-k_i^2/k_T^2}}{k_T^4} \cdot \Delta V_i$$

$$(16)\quad J_{\text{Detector}} \approx S(\vec{\kappa},\omega) \cdot \frac{e^{-k_i^2/k_T^2}}{k_T^4} \cdot \Delta V_i \cdot \Delta V_f \cdot$$

In a T. O. F. experiment as illustrated in Fig. 2, where the collimation or $\Delta\Omega_i$ is the same for all k_i, the momentum space volume ΔV_i is proportional to k_i^4 since

$$(17)\quad \frac{\Delta k_i^{(z)}}{k_i} = \frac{\Delta t}{t} = \frac{\Delta t}{\ell_i} \cdot v_i = \left[\frac{\Delta t}{\ell_i} \cdot \frac{\hbar}{m}\right] \cdot k_i = \text{const. } k_i$$

and

$$(18)\quad \Delta\Omega_i = \Delta k_i^{(x)} \cdot \Delta k_i^{(y)} / k_i^2$$

and therefore

$$(19)\quad \Delta V_i \approx \Delta\Omega_i \cdot k_i^4$$

The intensity at the target is therefore proportional to

$$(20)\quad J_{Target} \approx \frac{e^{-k_i^2/k_T^2}}{k_T^4} \cdot k_i^4 = e^{-E_i/E_T} \cdot \left(\frac{E_i}{E_T}\right)^2 = e^{-x} \cdot x^2$$

In Fig. 4 the relative intensity at the position of the target is plotted as a function of $x = E_i/E_T$. It can be seen that the intensity is a slowly varying function in a rather large energy range. Since in any neutron scattering experiment the resolution has to be adjusted to the neutron source strength, the T. O. F. -technique is an appropriate method for diffraction and neutron down-scattering experiments. The inverted statistical chopper facility as discussed in this context is a T. O. F. -spectrometer with special features. As it can be seen from Fig. 2, the distance Target-Crystal-Detector can be changed at will and therefore the resolution and intensity, determined by ΔV_f adjusted appropriately. From equation (16) it follows that the intensity distribution at the detector is determined by the static and dynamic structure of the target material. For down-scattering experiments with the target material at a temperature T for which $k_B \cdot T \ll \hbar\omega$, the intensity at the detector is determined by the double differential cross section or the scattering law $S(\vec{\kappa},\omega)$ which is given in the case of the harmonic oscillator by

$$(21)\quad \frac{d^2\sigma_{o-m}}{d\Omega_f dE_f} = \langle a^2 \rangle \frac{k_f}{k_i} e^{-\frac{k^2\langle u^2\rangle}{2}} \sum_{m=0}^{\infty} (\kappa^2\langle u^2\rangle)^m \delta(E_f - E_i + \hbar\omega_o \cdot m)$$

and for m = 1

$$(22)\quad \frac{d^2\sigma_{o-1}}{d\Omega_f dE_f} = \langle a^2 \rangle \frac{k_f}{k_i} \cdot e^{-\frac{k^2\langle u^2\rangle}{2}} \cdot (\kappa^2\langle u^2\rangle) \cdot \delta(E_f - E_i + \hbar\omega_o)$$

and

$$(23)\quad S(\vec{\kappa},\omega) = e^{-\frac{k^2\langle u^2\rangle}{2}} \cdot (\kappa^2\langle u^2\rangle) \cdot \delta(E_f - E_i + \hbar\omega_o)$$

The scattering law has an optimum at

$$(24)\quad \kappa^2_{opt} = \frac{2}{\langle u^2 \rangle}$$

where u stands for the oscillator amplitude. For the isotropic harmonic oscillator this amplitude can be calculated easily from

$$(25)\quad m\omega_o^2 \langle u^2 \rangle = \left[n(\omega_o) + \frac{1}{2} \right] . \hbar\omega_o$$

$$\langle u^2 \rangle = \frac{\hbar^2}{2m} \cdot \frac{1}{\hbar\omega_o}$$

where $n(\omega_o)$ stands for the Bose occupation number. The maximum intensity is therefore obtained in experiments with

$$(26)\quad \kappa^2_{opt} = \frac{2m}{\hbar^2} (2\hbar\omega_o).$$

Fig. 5 shows the κ^2-dependence of the scattering law of the isotropic harmonic oscillator. In a white neutron beam, with the intensity distribution as shown in Fig. 4, the optimum intensity condition can be obtained easily for any vibrational state and frequency distribution function. In a real experiment where multi-phonon processes occur, it is necessary to measure the energy transfer and the natural line shape as a function of κ^2 in the range $0 \leqslant \kappa^2 \leqslant \kappa^2_{opt}$ in order to eliminate the multiphonon contributions that lead to ambiguous results. Therefore it is desirable to collect data in a large space of the κ,ω-plane. For measurements concerning the density of state distribution function, where a large range of the possible energy transfer $\hbar\omega$ ought to be measured at small κ-values, the white neutron beam experiment is most suitable. It may be mentioned that the energy calibration of the crystal spectrometer and the determination of the reflectivity of the crystals can be done by using a Vanadium target and the time of flight spectrometer of the inverted statistical chopper facility. The detector

efficiency has to be determined only for one neutron energy. No mechanical drive systems are needed for the crystal spectrometer.

II. 2 Comparison of a Conventional and an Inverted Statistical Chopper Facility

II. 2. 1 - The κ,ω-range of the two instruments

In Fig. 6 and Fig. 7 the two cases in question are illustrated in real- and momentum space representation. The flexibility of the two instruments can be characterized by the corresponding κ,ω-range, the resolution function and the intensity in this region. From Fig. 1 and the conservation of energy

$$(27)\quad \hbar\omega = \frac{\hbar^2}{2m}\left(k_i^2 - k_f^2\right)$$

follows for the inverted statistical chopper

$$(28)\quad \hbar\omega = \frac{\hbar^2}{2m}\left[2(\vec{\kappa},\vec{k}_i) - \kappa^2\right] = E_i - E_f =$$

$$= \frac{\hbar^2}{2m}\left[2k_f \cdot \cos\vartheta \cdot \sqrt{\kappa^2 - k_f^2 \sin^2\vartheta} - 2k_f^2 \sin^2\vartheta + \kappa^2\right]$$

and for the conventional statistical chopper

$$(29)\quad \hbar\omega = \frac{\hbar^2}{2m}\left[2k_i^2 \cdot \sin^2\vartheta \pm 2k_i\left\{k_i^2 \cdot \sin^2\vartheta(\sin^2\vartheta - 1) + \cos^2\vartheta \cdot \kappa^2\right\}^{1/2} - \kappa^2\right]$$

Using these equations, the κ,ω-range can be calculated and is shown in Fig. 8, 9 and 10. For the inverted case the κ,ω-region is given for a pyrolytic graphite, a Be-single crystal and a Be-MgO window filter in the analyser spectrometer. The inverted spectrometer has an "open" region towards large κ,ω-values and collects most of the data in a region with low κ-values. This feature remains even if k_i is enlarged for the conventional case (a typical case

has been chosen). It is important to avoid large data collection in regions with high multiphonon background.

II. 2. 2 - The Resolution-functions of the inverted and conventional statistical chopper facility

The relative error of an energy transfer $\hbar\omega$ -measurement is given by

$$(30)\quad \frac{\Delta\hbar\omega}{\hbar\omega} = \frac{2k_i \cdot \Delta k_i + 2k_f \cdot \Delta k_f}{k_i^2 - k_f^2}$$

Since for an inverted time of flight spectrometer

$$(31)\quad \Delta k_i = \frac{\Delta t}{\ell_i} \cdot \frac{\hbar}{m} \cdot k_i^2$$

the resolution function of the inverted facility is given by

$$(32)\quad \frac{\Delta\hbar\omega}{\hbar\omega} = \left[\frac{2\Delta t}{\ell_i} \cdot \frac{\hbar}{m} \cdot \frac{\hbar^2}{2m}\right] \frac{\left\{\frac{2m}{\hbar^2}(\hbar\omega) + k_f^2\right\}^{3/2}}{\hbar\omega} + \frac{\frac{\hbar^2}{2m} \cdot 2k_f \cdot \Delta k_f}{\hbar\omega}$$

where

$$(33)\quad \Delta t = \left\{\Delta t_{St.Ch.}^2 + \left(\frac{\ell_f}{\frac{\hbar}{m} \cdot k_f} \cdot \frac{\Delta k_f}{k_f}\right)^2\right\}^{1/2}$$

and for the conventional case by

$$(34)\quad \frac{\Delta\hbar\omega}{\hbar\omega} = \left[\frac{\Delta t_{St.Ch}}{\ell_f} \cdot \frac{\hbar}{m} \cdot \frac{\hbar^2}{2m}\right] \frac{\left\{k_i^2 - \frac{2m}{\hbar^2}(\hbar\omega)\right\}^{3/2}}{\hbar\omega} + \frac{\frac{\hbar^2}{2m} \cdot 2k_i \cdot \Delta k_i}{\hbar\omega}$$

In Fig. 11, 12, 13, 14 and 15 the resolution functions are given for various sets of $k_i \cdot \Delta k_i$, $k_f \cdot \Delta k_f$ and Δt with $\ell_i^{I.Ch.} = 15$ m and $\ell_f^{C.Ch.} = 4$ m. The resolution functions of the conventional case show a strong dependence

on $\hbar\omega$ since small $\hbar\omega$-values are measured as the difference of two large numbers, demonstrating clearly the disadvantage of the conventional facility. Limiting in this case the accessible region in the κ,ω-plane by chosing small k_i-values, of course any value $\hbar\omega$ can be measured with the requested energy resolution compatible with the available source strength. However, this procedure costs time and money.

II. 2. 3 - Comparison of the intensity of the two instruments

In Fig. 8, 9 and 10 it is demonstrated that the accessibility in the κ,ω plane is quite different for the two instruments and in Fig. 11-15 it is shown that the energy resolution functions are again very different for a given range of $\hbar\omega$. Therefore the performance characteristics of the two instruments are quite different for a certain setting of k_i, Δk_i and k_f, Δk_f-values. Consequently, a comparison of the intensity in a certain κ,ω-range is not possible. Hence we limit our considerations to two cases:

1. $\hbar\omega = 150$ meV $\pm$ 5.4% and $\kappa = 4.88$ Å^{-1} $\pm$ 3.1%

and

2. $\hbar\omega = 150$ meV $\pm$ 4.5% and $\kappa_{I.Ch} = 8.75$ Å^{-1} $\pm$ 23%

and $\kappa_{C.Ch} = 8.75$ Å^{-1} $\pm$ 6.14%

For the second case with large momentum transfer it is assumed that in the conventional spectrometer neutrons are detected between $0^\circ \leqslant \vartheta \leqslant 90^\circ$ and in the inverted spectrometer in a 4π-Be-MgO window filter detector. In this case experiments are compared that have the same energy resolution but different and possible $\vec{\kappa}$-resolutions.

It is assumed that the conventional spectrometer has straight detectors from 0° to 90° scattering angle, a detector length of 1.4 m and a flight path

of 4 m, defining a $\Delta\beta_f = \frac{1.4}{4} = 0.35 \approx 20^o$. This is about the limit for straight detectors for which

$$(35) \quad \sin(\tfrac{1}{2}\Delta\beta_f) \lessapprox \sqrt{\frac{\Delta k_f^{(z)}}{k_f}}$$

The detectors of the inverted spectrometer have a length of 0.7 m and are positioned 2 m (ℓ_f) from the target. For reasons concerning the resolution the distance target-detector (ℓ_f) or $\Delta\beta_f$ must fulfil the following condition

$$(36) \quad \cos(\tfrac{1}{2}\Delta\beta_f) \lessapprox \frac{1 - \frac{\Delta k_f^{(z)}}{k_f}}{1 + \frac{\Delta k_f^{(z)}}{k_f} \cdot \tan^2\alpha}$$

where α denotes the Bragg angle.

For optimum intensity and accuracy one chooses for this particular comparison for both cases $k_i . \Delta k_i = k_f . \Delta k_f$. In general the intensity ratio of the inverted and conventional spectrometers is taken as the figure of merit:

$$(37) \quad M(\hbar\omega, \kappa) = \frac{\left[R(k_f) . \varepsilon(k_f) . F_T . e^{-k_i^2/k_T^2} . \Delta V_i . \Delta V_f\right]_{\text{I. Ch.}}}{\left[R^2(k_i) . \varepsilon(k_f) . F_T . e^{-k_i^2/k_T^2} . \Delta V_i . \Delta V_f\right]_{\text{C. Ch.}}}$$

where R(k) stands for the reflectivity of the corresponding crystals and neutron energy and $\varepsilon(k_f)$ for the detector efficiency.

For the conventional spectrometer a variable k_i is mandatory and consequently a double crystal spectrometer must be installed since the large detector installation cannot be moved. The figure of merit must be calculated under the boundary conditions

$$(38)\quad \left[\frac{\Delta\hbar\omega}{\hbar\omega}(K,\omega)\right]_{C.Ch.} = \left[\frac{\Delta\hbar\omega}{\hbar\omega}(K,\omega)\right]_{I.Ch.}$$

and

$$(39)\quad \left[\frac{\Delta K}{K}(K,\omega)\right]_{C.Ch.} = \left[\frac{\Delta K}{K}(K,\omega)\right]_{I.Ch.}$$

Assuming no limitations in sample size (a reasonable assumption for incoherent down-scattering experiments) and equal detector efficiency equation (37) reduces for these particular cases to

$$(40)\quad M(\hbar\omega, K) = \frac{\left[R(k_f).F_T.\Delta V_i.\Delta V_f\right]_{I.Ch.}}{\left[R^2(k_i).F_T.\Delta V_i.\Delta V_f\right]_{C.Ch.}} \quad .$$

The figure of merit is determined by calculating the possible momentum space elements imposed by the geometrical conditions of the two spectrometers and equations (35), (36), (38) and (39). In spite of these boundary conditions, the volume elements and their product may be quite different.

In Table 1 and 2 the characteristic performance data for the two cases are summarized.
For the first case we obtain:

$$M = 1.12$$

and for the second case:

$$M = 14.4 \quad .$$

From the results, the large accessibility in the K,ω-plane, the wide range of the flat resolution function and the possibility of a 4π-detector system, it is concluded that the inverted spectrometer is very suitable for down-scattering experiments and unique for the determination of line shapes and widths.

Parameters	$\hbar\omega$	$\frac{\Delta\hbar\omega}{\hbar\omega}$	K	$\frac{\Delta K}{K}$	k_i	$\frac{\Delta k_i}{k_i}$	k_f	$\frac{\Delta k_f}{k_f}$	l_i	l_f	Δt St.Ch.	Δt	$\Delta\alpha_i$	$\Delta\beta_i$	$\Delta\Omega_i$	ΔV_i
Dimensions	meV	%	$\mathring{A}^{-1}$	%	$\mathring{A}^{-1}$	%	$\mathring{A}^{-1}$	%	m	m	μ sec.	μ sec.	Rad 10^3	Rad 10^3	Sterad 10^6	$\mathring{A}^{-3}$ 10^6
Inverted Spectrometer	150	5,41	4,88	3,1	10	1,17	5,29	3,06	15	2	20	27	0,6667	3,333	2,22	25,9
Conventional Spectrometer	150	5,41	4,88	3,1	10	1,09	5,29	3,06	0	4	36,5		2,15	20	43	469

Parameters	$\Delta\alpha_f$	$\Delta\beta_f$	$\Delta\Omega_f$	ΔV_f		F_T	R_{Be}	ϑ	α_{Be}	$\Delta\alpha_{Be}$		$\frac{\Delta V_f}{\Delta V_i}$	$\frac{\Delta\Omega_f}{\Delta\Omega_i}$			
Dimensions	Rad $x10^3$	Rad $x10^3$	Sterad $x10^6$	$\mathring{A}^{-3}$ $x10^6$		Cm^2	%	Degree	Degree	Rad $x10^3$						
Inverted Spectrometer	11,1	700	7777	35200		15x3	0,5	10,2	20	11,1		1360	3500			
Conventional Spectrometer	30	350	10500	48500		5x1	0,4	10,2	10,41	2,15		103	244			

$M(\hbar\omega, k) = 1.12$

Tab.1 THE CHARACTERISTIC PERFORMANCE DATA FOR THE TWO SPECTROMETERS FOR $\hbar\omega = 150$ meV ± 5,41 % AND $K = 4{,}88\ \mathring{A}^{-1}$ ± 3,1 %

Parameters	$\hbar\omega$	$\frac{\Delta\hbar\omega}{\hbar\omega}$	K	$\frac{\Delta K}{K}$	k_i	$\frac{\Delta k_i}{k_i}$	k_f	$\frac{\Delta k_f}{k_f}$	l_i	l_f	$\Delta t_{St.Ch.}$	Δt	$\Delta\alpha_i$	$\Delta\beta_i$	$\Delta\Omega_i$	ΔV_i
Dimensions	meV	%	$\mathring{A}^{-1}$	%	$\mathring{A}^{-1}$	%	$\mathring{A}^{-1}$	%	m	m	μ sec.	μ sec.	Rad $\times 10^3$	Rad $\times 10^3$	Sterad $\times 10^6$	$\mathring{A}^{-3}$ $\times 10^6$
Inverted Spectrometer	150	4,5	8,75	23	8,62	2,01	1,54	6,14	15	0,6	40	55	0,6667	3,3333	2,22	29
Conventional Spectrometer	150	4,5	8,75	6,14	8,62	1,9	1,54	6,14	0	4	250	250	4,1	20	82	1060

Parameters	$\Delta\alpha_f$	$\Delta\beta_f$	$\Delta\Omega_f$	ΔV_f		F_T	R_{Be}	ϑ	α_{Be}	$\Delta\alpha_{Be}$	Tr_{Be}		$\frac{\Delta V_f}{\Delta V_i}$	$\frac{\Delta\Omega_f}{\Delta\Omega_i}$		
Dimensions	Rad	Rad	Sterad	$\mathring{A}^{-3}$		Cm^2	%	Degree	Degree	Rad $\times 10^3$	%					
Inverted Spectrometer	2π	2π	4π	2,81		15 x 3		$0°$ – $360°$	-	-	0,8		9,69 $\times 10^4$	5,66 $\times 10^6$		
Conventional Spectrometer	1,57	0,35	0,55	8×10^2		5	0,4	$0°$ – $90°$	12,1	1,51			75,4	6700		

$M(\hbar\omega) = 14,4$

Tab. 2 THE CHARACTERISTIC PERFORMANCE DATA OF THE TWO SPECTROMETERS FOR $\hbar\omega = 150$ meV ± 4,5 % AND $K = 8,75\ \mathring{A}^{-1}$ (I.CH. ± 23 %; C.CH. ± 6 14 %)

III. Fields of Application

A white neutron beam experiment as discussed in this context has a wide range of application. In diffraction experiments most of the lines appear in backscattering directions well accessible in the geometry of an inverted spectrometer. For the analysis of complex structures large numbers of lines have to be measured and a wide K-range is requested. As illustrated in Fig. 17, this can be done at the inverted spectrometer. For certain experiments concerning phase transitions, it is of interest to measure simultaneously as a function of temperature, pressure, electric and magnetic fields the static structure, phonons and frequency density distributions.

For the study of the dynamics of hydrogen impurities in metals it is mandatory to measure simultaneously and possibly in single crystals the local modes, their line width and line shape, the band mode frequency distribution function and the quasi-elastic line. Measurements concerning these problems are performed in the best manner at a white neutron beam spectrometer with constant resolution function. The same arguments are practically valid for all incoherent scattering experiments important for the study of hydrogenous materials. To a certain extent the inverted spectrometer is of interest in neutron radiography for non-destructive test experiments.

IV. The Theory of the Inverted Statistical Chopper Facility

In this chapter we describe:

1) how to perform the cross-correlation between the (pseudostatistical) on- and off-pattern of the statistical chopper and the number of counts in the different analyser channels;

2) how to extract information about the scattering function out of the measured correlation function and consider

3) the influence of the statistical error of the counts in the analyser channels on the statistical accuracy of the (measured) scattering function.

The argumentation is based on the method and results presented in the papers [9] and [16].

For an analytical description of the chopper-sample-detector configuration we measure the time at the chopper and detector position in intervals of equal length Θ and introduce the quantities:

$$q_1 = \begin{cases} 1 \text{ if the chopper was open in time interval i} \\ 0 \text{ if the chopper was closed in time interval i} \end{cases}$$

$Q(i)$ number of detector counts in time interval i if the chopper was open in time interval "0" only

$C(k)$ total number of detector counts in time interval k (detector channel k)

$b(k)$ total number of background counts in detector channel k (assumed to be independent of k: $b(k) = b$)

Then we have:

$$(41) \quad C(k) = \sum_{i=-\infty}^{+\infty} a_{k-i} Q(i) + b(k)$$

As the statistical chopper works periodically in time with period $N\theta$, we have

$$(42) \quad a_i = a_i \pm \ell N \qquad (\ell = 1, 2, \ldots)$$

Furthermore the sequence a_i is chosen to have the pseudostatistical property:

$$(43) \quad \sum a_i a_{i+\ell} = m(1-c)\, \delta_{\ell \bmod(N)} + mc$$

where m is the number of times for which $a_i = 1$ within one period and $c = (m-1)/(N-1)$.

After measuring over K periods we perform the correlation operation:

$$(44) \quad \sum_{i=1}^{KN} a_i C(i+k) = \sum_{i=1}^{N} a_i \sum_{\ell=0}^{K-1} C(i+\ell N+k)$$

Denoting the sum of the detector counts in corresponding channels over K periods again by C(i+k) we obtain, under the assumption that

$$(45) \quad Q(i) \begin{cases} \neq 0 & \text{for } 1 \leqslant i \leqslant N \\ = 0 & \text{for } N < i \end{cases}$$

the result:

$$(46) \quad \sum_{i=1}^{N} a_i C(i+k) = Km(1-c)Q(k) + KmcQ + Kbm$$

where

$$(47) \quad Q = \sum_{i=-\infty}^{+\infty} Q(i)$$

On the other hand we have:

$$(48) \quad \sum_{i=1}^{N} c(i+k) = KmQ + KNb$$

Combining this expression with (47) gives us finally

$$(49)\quad Q(k) = \frac{1}{Km(1-c)} \sum_{i=1}^{N} (a_i - c).C(i+k) - \frac{b}{m}$$

As the C(i) are statistically independent quantities with a Poisson distribution, we obtain for the variance of Q(k)

$$(50)\quad \sigma^2_{Q(k)} = \frac{Q(k)+b}{K} \cdot \frac{N^{-1} + c\alpha^{-1}(k)}{(1-c)mN^{-1}}$$

with

$$(51)\quad \alpha(k) = \frac{N(Q(k)+b)}{Q - 2Q(k) - \frac{b}{m}}$$

The first factor in (50) is just the variance of Q(k) if the measurement would have been performed in the conventional way using K pulses of width θ. This leads us to write:

$$(52)\quad G^2(k) \left\{\sigma^2_{Q(k)}\right\}_{\substack{\text{statistical}\\ \text{chopper}}} = \left\{\sigma^2_{Q(k)}\right\}_{\substack{\text{conventional}\\ \text{chopper}}}$$

where

$$(53)\quad G^2(k) = \frac{(1-c)mN^{-1}}{N^{-1} + c\alpha^{-1}(k)}$$

can be interpreted as a gain factor, indicating that the statistical chopper is superior to the conventional chopper when $G^2 > 1$.

A detailed parameter study of G was made by Scherm [16], who showed that basically $G^2(k)$ will be larger than one, if $\alpha(k)$ is larger than one. The discussion of the gain factor $G^2(k)$ reduces therefore to a discussion of $\alpha(k)$, especially to the determination of those parts of Q(k) in which $\alpha(k)$ is larger than one. For this investigation we assume further $N \gg 1$ and we may neglect

b/m and Q(k) compared to Q.

Then we obtain:

$$(54)\quad \alpha(k) \approx \frac{Q(k) + b}{\bar{Q}}$$

$$(55)\quad \bar{Q} = \frac{1}{N} \sum_{i=1}^{N} Q(i)$$

This is the well known result, that for stationary neutron beams the statistical chopper is superior to the conventional one for those parts of Q(k) for which $\alpha(k)$ is larger than one and that this part is determined by the mean value $\bar{Q}$ of the whole spectrum Q(k).

Now we turn to the discussion of the function Q(k) for two special time of flight experiments:

a) input energy fixed (normal chopper, Fig. 17 a),
b) output energy fixed (inverted chopper, Fig. 17 b).

With the normal (statistical) chopper neutrons of fixed energy E^* enter the chopper-sample-detector system during time interval 0 at the position of the (statistical) chopper.
The target is just behind the chopper.
The scattered neutrons after the target have different energies and arrive in different time-intervals k at the detector.
In this case we have:

$$(56)\quad Q(k) = M(E^*) \cdot S(E^*, k)$$

where

$M(E^*)$ is the total number of neutrons (with an energy in the interval ΔE^* around E^*) entering the system during interval "0".

$S(E^{\pm}, k)$ is the probability that a neutron (out of the input pulse) of energy $E^{\pm}$ generates a count in the detector channel k .

With the inverted (statistical) chopper neutrons out of a white spectrum enter the system during time interval "0" at the position of the (statistical) chopper.

The target is just before the detector.
The incoming neutrons have different energies and arrive at different time-intervals k at the target.
In this case we have

$$(57) \quad Q^{+}(k) = M(k).\, S(k, E^{\pm})$$

where:

$M(k)$ is the total number of neutrons arriving at the target in time interval k

$S(k, E^{\pm})$ is the probability that a neutron arriving in time interval k at the target will generate a count in the detector after scattering into the energy (-interval $\Delta E^{\pm}$ around) $E^{\pm}$.

If we denote by

$I(E)\Delta E$ the intensity of the incoming neutrons with energy in ΔE around E, by

$S(E, E')\Delta E'$ the scattering probability for a neutron from energy E into the interval $\Delta E'$ around E' (for the scattering-geometry chosen), and by

$E(\tau)$ the energy necessary for a neutron to cover the flight path from the chopper to the detector in time τ

then we have for both cases:

$$(58) \quad Q(k) = I(E^{\pm}).\, S(E^{\pm}, E)\frac{\partial E}{\partial \tau}\, \Delta E^{\pm} \theta^{2}$$

$$(59)\quad Q^{+}(k) = I(E).S(E, E^{*}) \frac{\partial E}{\partial \tau} \Delta E^{*} \theta^{2}$$

If a Maxwellian spectrum is used for the experiments, the principle of detailed balance:

$$(60)\quad I(E^{*})S(E^{*}, E) = I(E)S(E, E^{*})$$

says that both experiments give us the same information and from the point of view of the statistical error they are equivalent.

Note that in the definition of the quantities entering equations (58) and (59) we put the resolution-functions for the incoming and outgoing neutrons equal to one for both versions of the statistical chopper. This is not correct, but the relative merits of the resolution functions for both types of statistical choppers is discussed in the other chapters of this paper.

V. Conclusions

It has been shown that the inverted time of flight spectrometer has a large accessibility in the κ,ω-plane and that the energy resolution function and the intensity is rather constant over a large energy range. The inverted geometry is therefore very favourable to perform precision measurements of line width and line shape of local modes, high energy phonons and magnons. In principle a 4π-Be-filter-detector can be built for high intensity low background experiments. The role of the statistical chopper is primarily to reduce the continuous elastic and inelastic background. All the results concerning the merits or advantages of a conventional statistical chopper compared to a common time of flight spectrometer are of course as valid for the inverted spectrometer.

In view of the above, we state that the inverted statistical chopper facility is a useful and interesting spectrometer for high energy transfer measurements as well as for high resolution powder diffraction work.

VI. Literature

/1/ BECKURTS, K.H., Kernforschungszentrum Karlsruhe, KFK, Internal Report (1968)

/2/ SKØLD, K., Nucl. Instrum. Meth., 63, 114 (1968), Nucl. Instrum. Meth., 63, 347 (1968)

/3/ PAL, L., KROÓ, N., PELLIONISZ, P., SZLARIK, F., VIZI, I., Neutron Inelastic Scattering Meeting, IAEA-Proceedings Symposium, Copenhagen, Vol. 2, 407 (1968)

/4/ GOMPF, F., REICHARDT, W., GLAESSER, W., BECKURTS, K.H., Neutron Inealstic Scattering Meeting, IAEA-Proceedings Symposium, Copenhagen, Vol. 2, 417 (1968)

/5/ HOSSFELD, F., AMADORI, R., SCHERM, R., IAEA-Proceedings of the Panel Conference on Instrumentation for Neutron Inelastic Scattering Research, Vienna, (1970)

/6/ HOSSFELD, F., AMADORI, R., KFA-Jülich-Report 684-FF, (1970)

/7/ KROÓ, N., IAEA-Proceedings of the Panel Conference on Instrumentation for Neutron Inelastic Scattering Research, Vienna (1970)

/8/ KLEY, W., Proceedings of the Joint Euratom-Japanese Information Meeting on the Design Status and the Projected Use in Science and Technology of the Euratom Project SORA and the Japanese LINAC-Booster Project, held at Ispra on Sept. 17-18, (1971), EUR-4954 e

/9/ MATTHES, W., IAEA-Proceedings Symposium, Grenoble, Neutron Inelastic Scattering, March 6-10 (1972)

/10/ AMADORI, R., HOSSFELD, F., Symposium Grenoble, Neutron Inelastic Scattering, March 6-10 (1972) 747

/11/ KROÓ, N., PELLIONISZ, P., VIZI, I., ZSIGMOND, G., ZHUKOV, G., NAGY, G., Inelastic Scattering, March 6-10 (1972) 763

/12/ PELLIONISZ, P., KROÓ, N., MAZEI, F., Inelastic Scattering, March 6-10 (1972) 787

/13/ KLEY, W., EUR-Report in print

/14/ KLEY, W., EUR-Report in print

/15/ MAIER-LEIBNITZ, H., Nukleonik, 8 (1966) 61

/16/ Von JAHN, R., SCHERM, R., Nuclear Instruments and Methods 80 (1970) 69

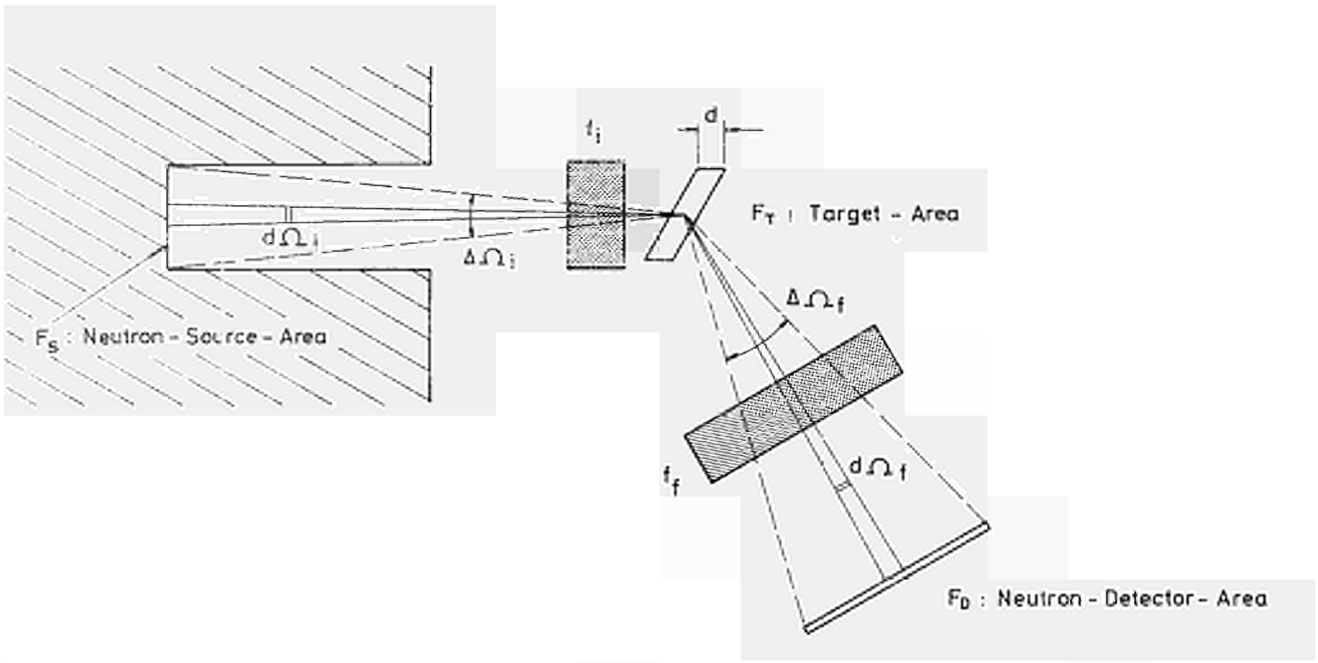

Fig. 1 GEOMETRICAL REPRESENTATION OF A NEUTRON SCATTERING EXPERIMENT

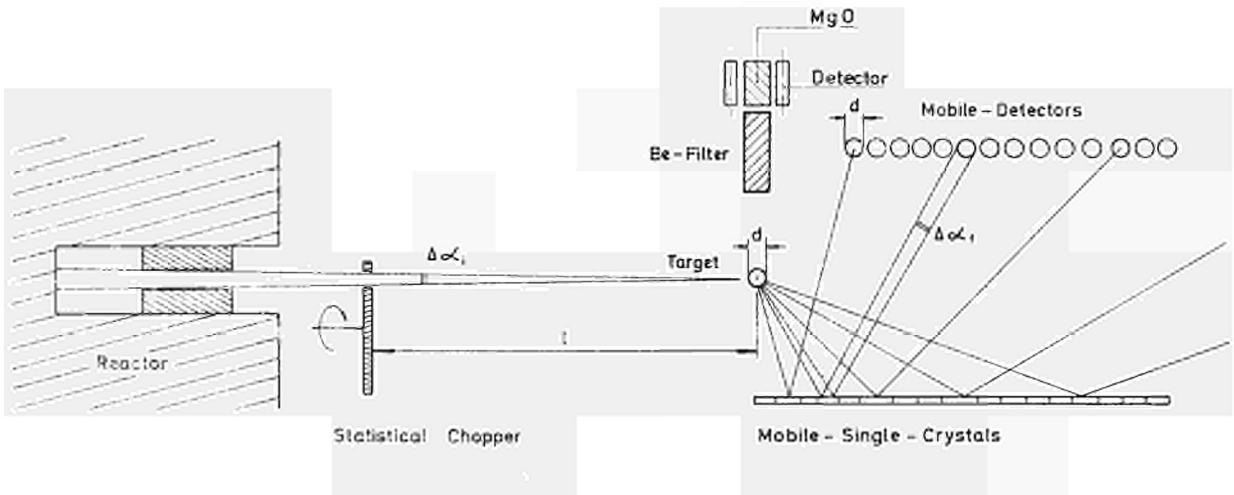

Fig. 2 THE INVERTED STATISTICAL CHOPPER FACILITY

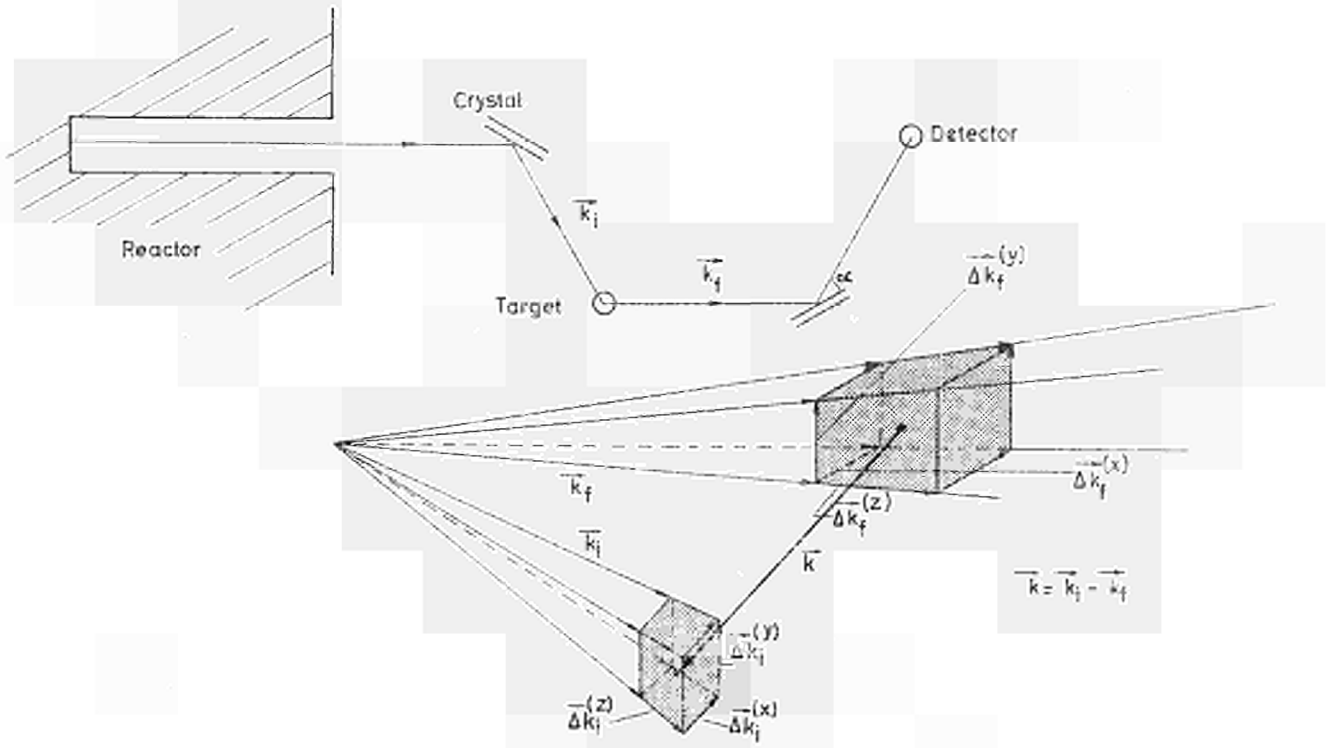

Fig.3. A NEUTRON SCATTERING EXPERIMENT WITH MONOCHROMATIC NEUTRON BEAMS IN REAL- AND MOMENTUM-SPACE

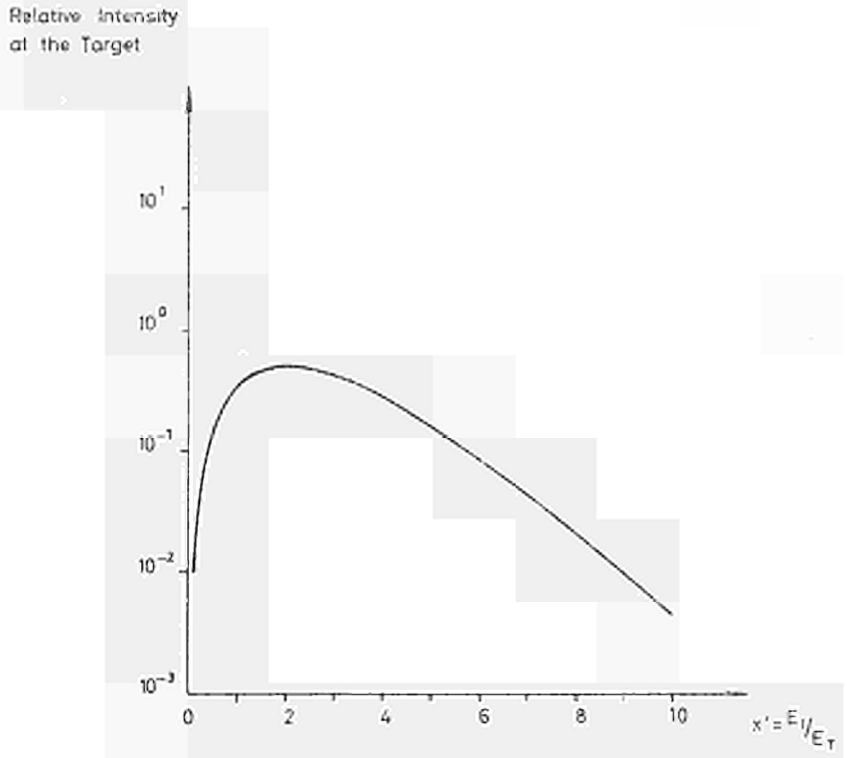

Fig 4 THE RELATIVE INTENSITY AT THE TARGET AS A FUNCTION OF THE RELATIVE NEUTRON ENERGY $x' = E_i / E_t$

$E_T = K_B \cdot T$ (K_B = Boltzmann - Constant ; T = Moderator - Temperature)

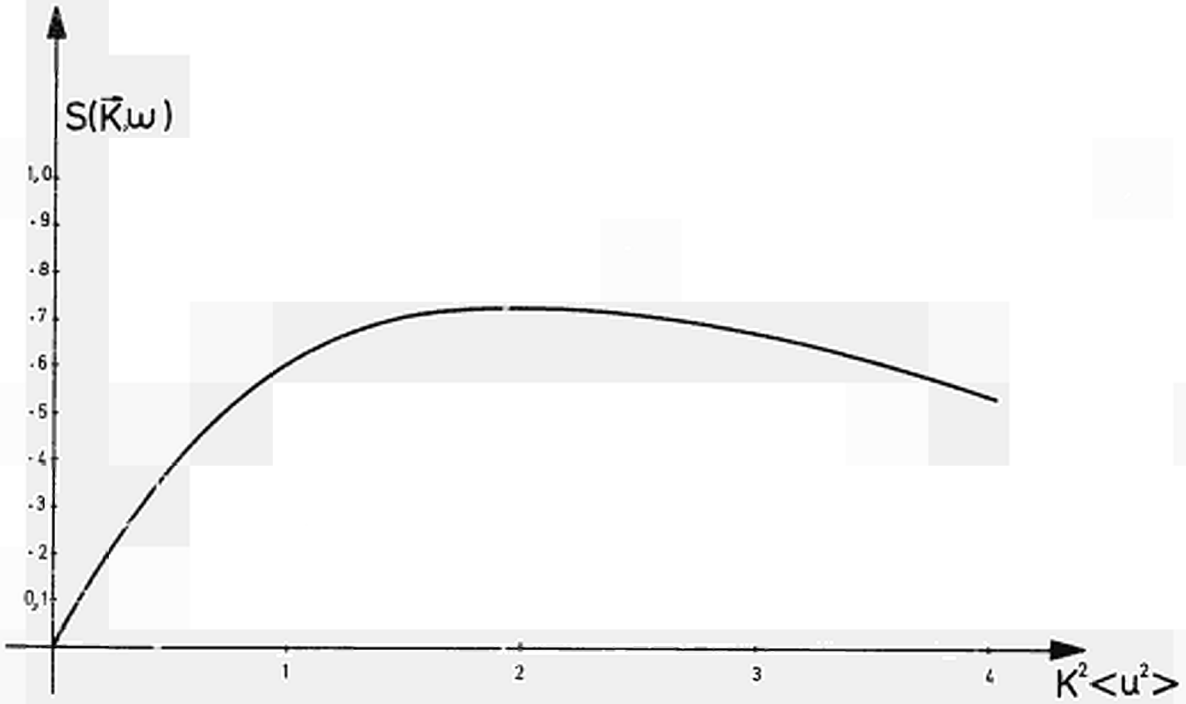

Fig. 5 The Scattering Law of an iso tropic harmonic oscillator

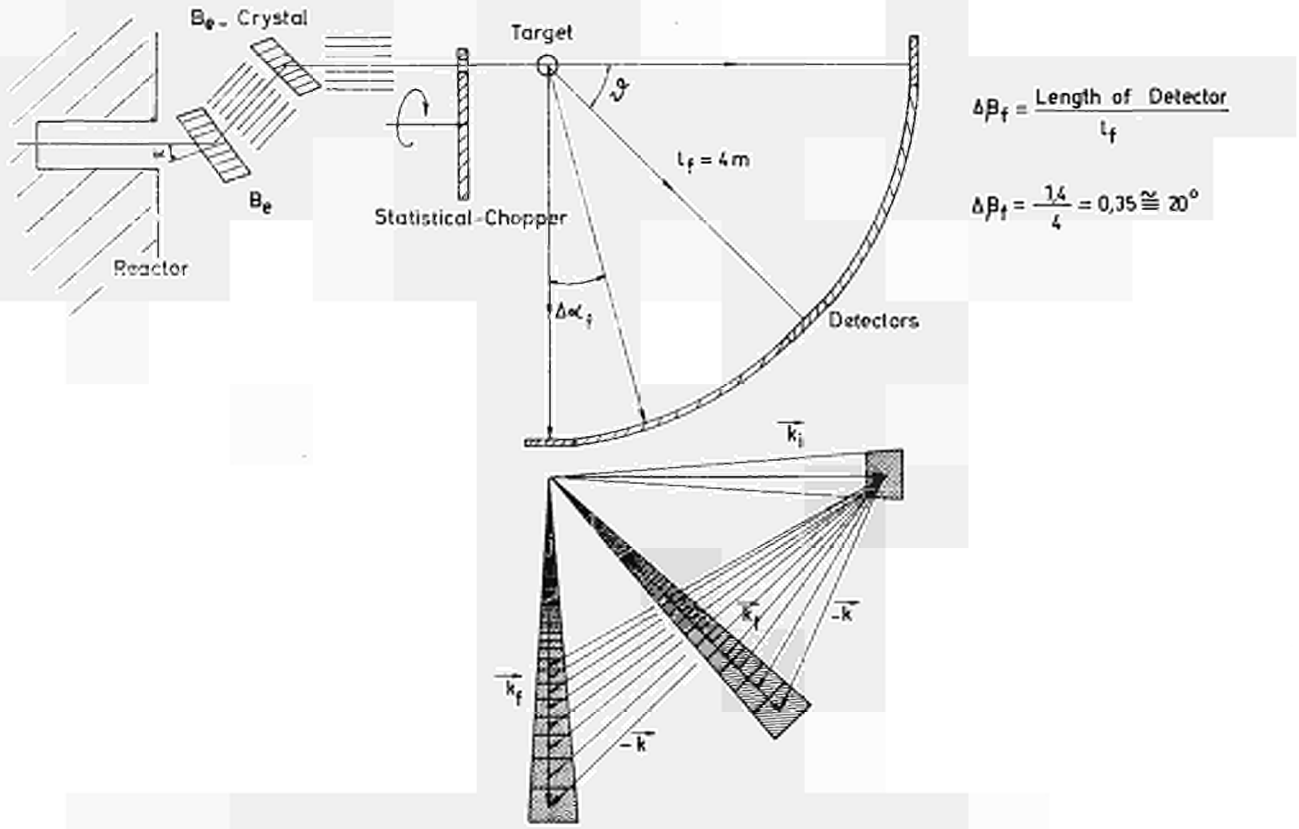

Fig.6 THE CONVENTIONAL STATISTICAL CHOPPER IN REAL- AND MOMENTUM-SPACE

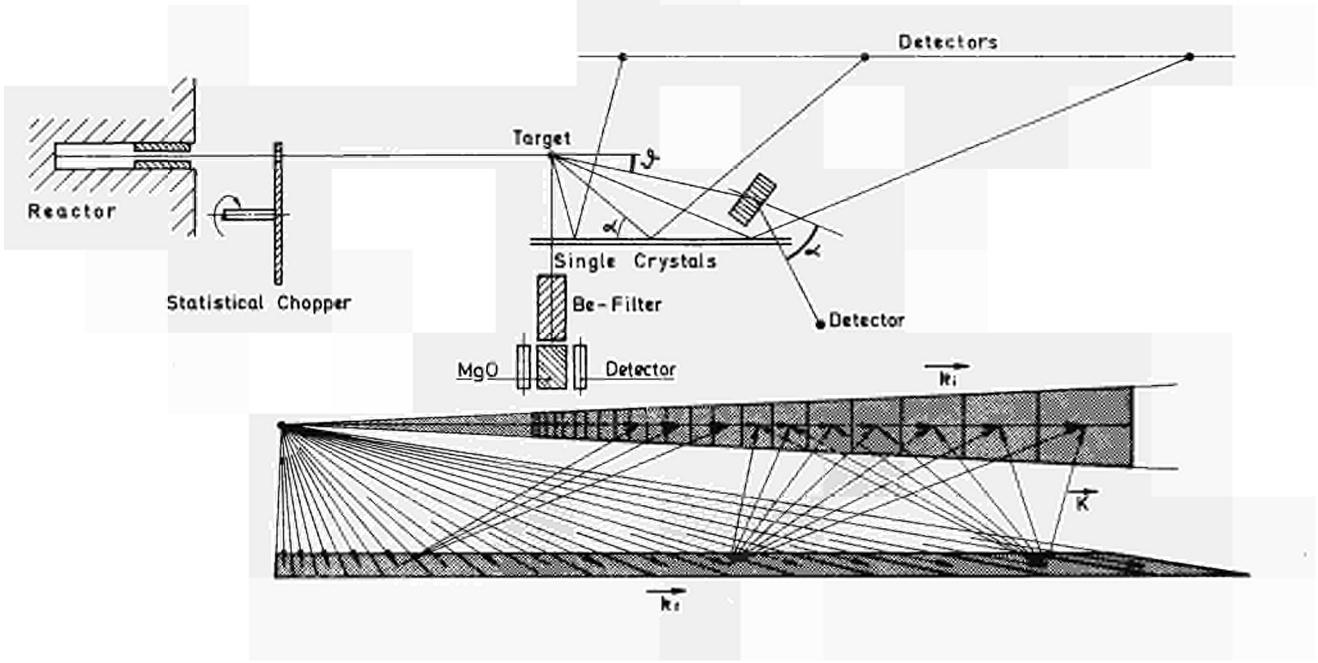

FIG. 7 - THE INVERTED STATISTICAL CHOPPER IN REAL- AND MOMENTUM - SPACE

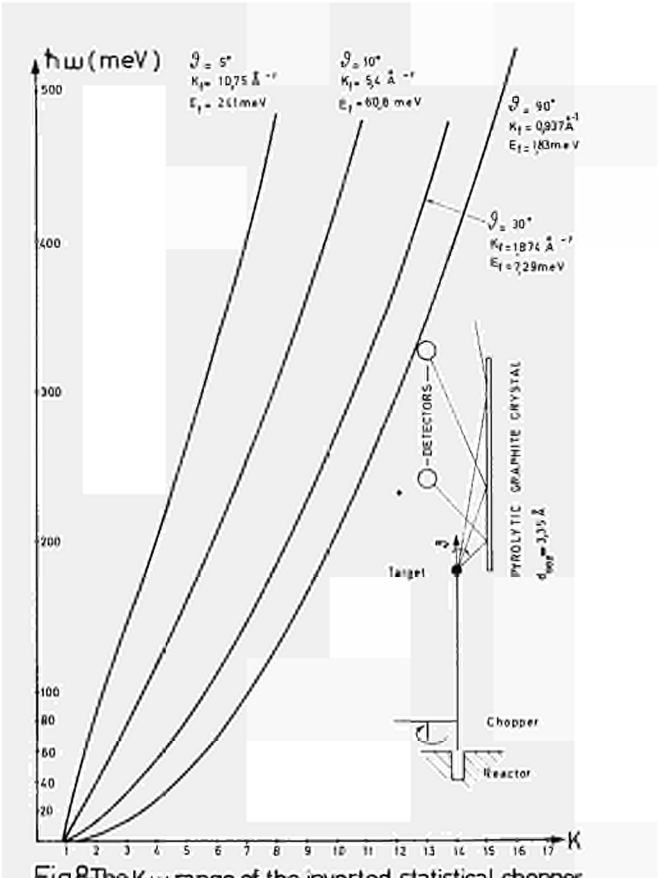

Fig.8 The K,ω range of the inverted statistical chopper

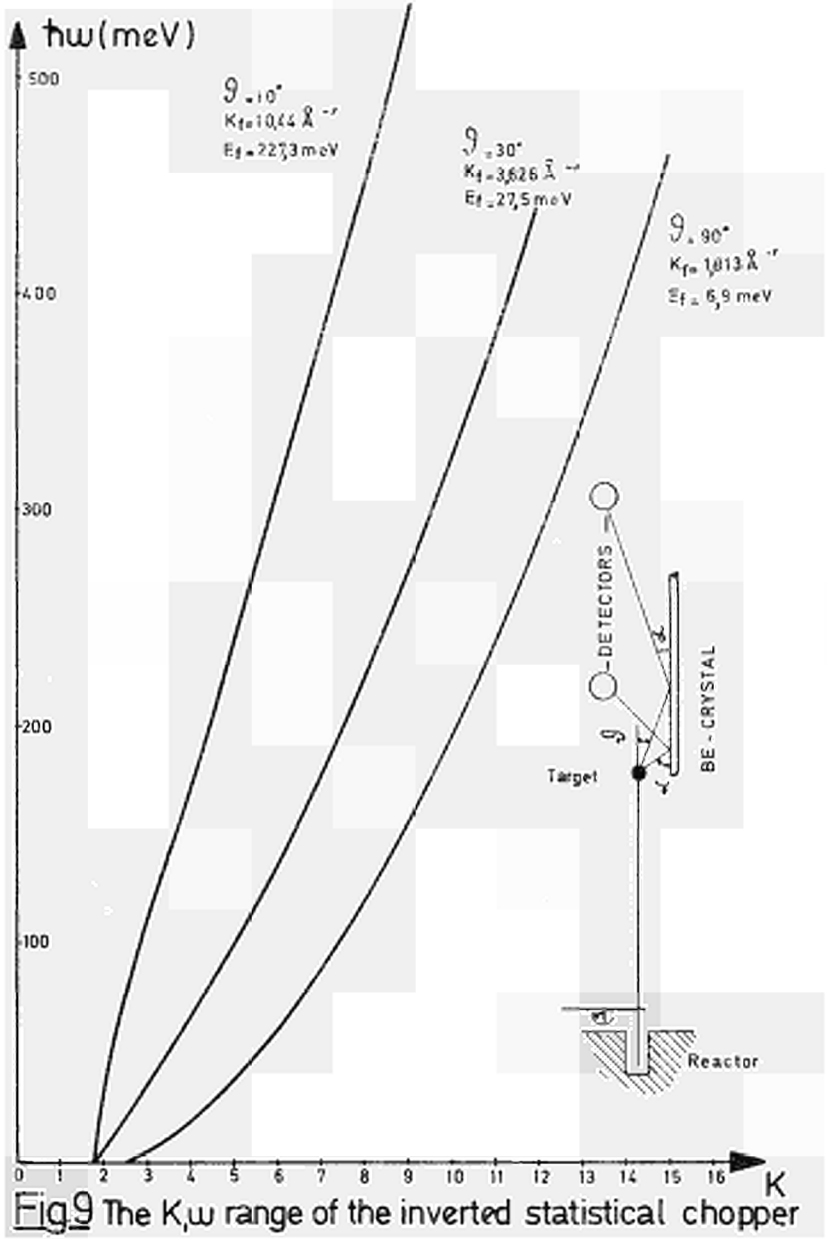

Fig.9 The K,ω range of the inverted statistical chopper

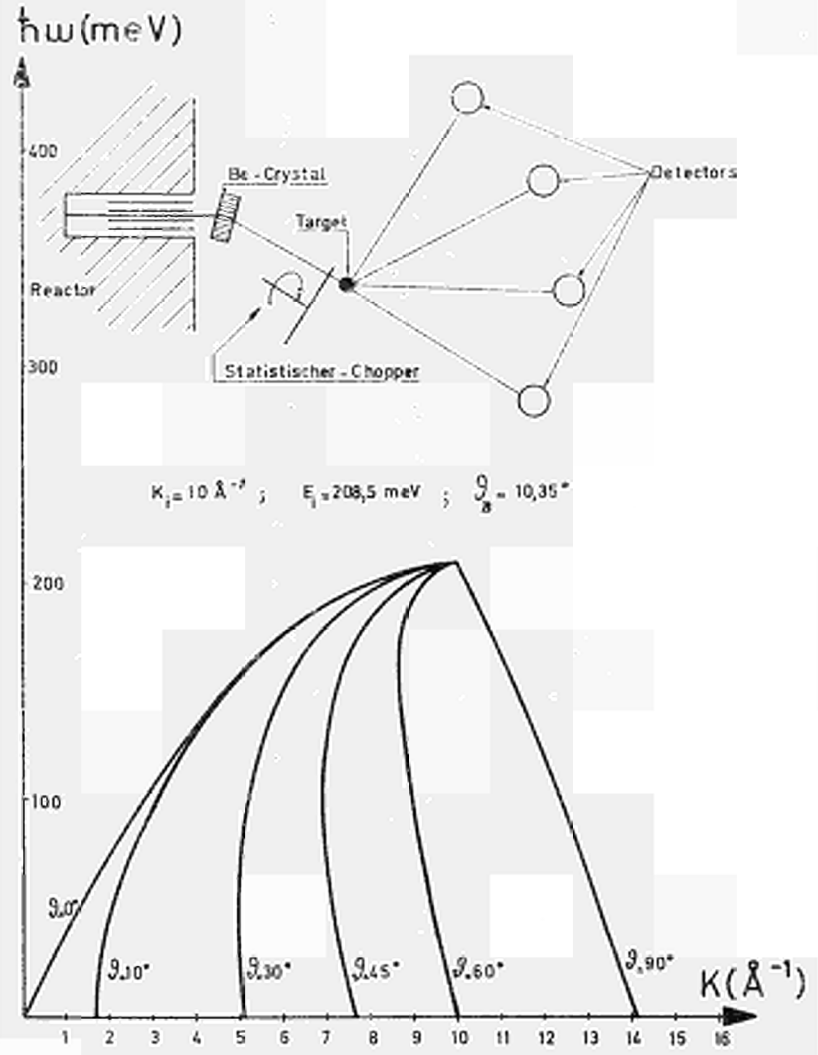

Fig.10 The K,ω range of the conventional statistical chopper facility

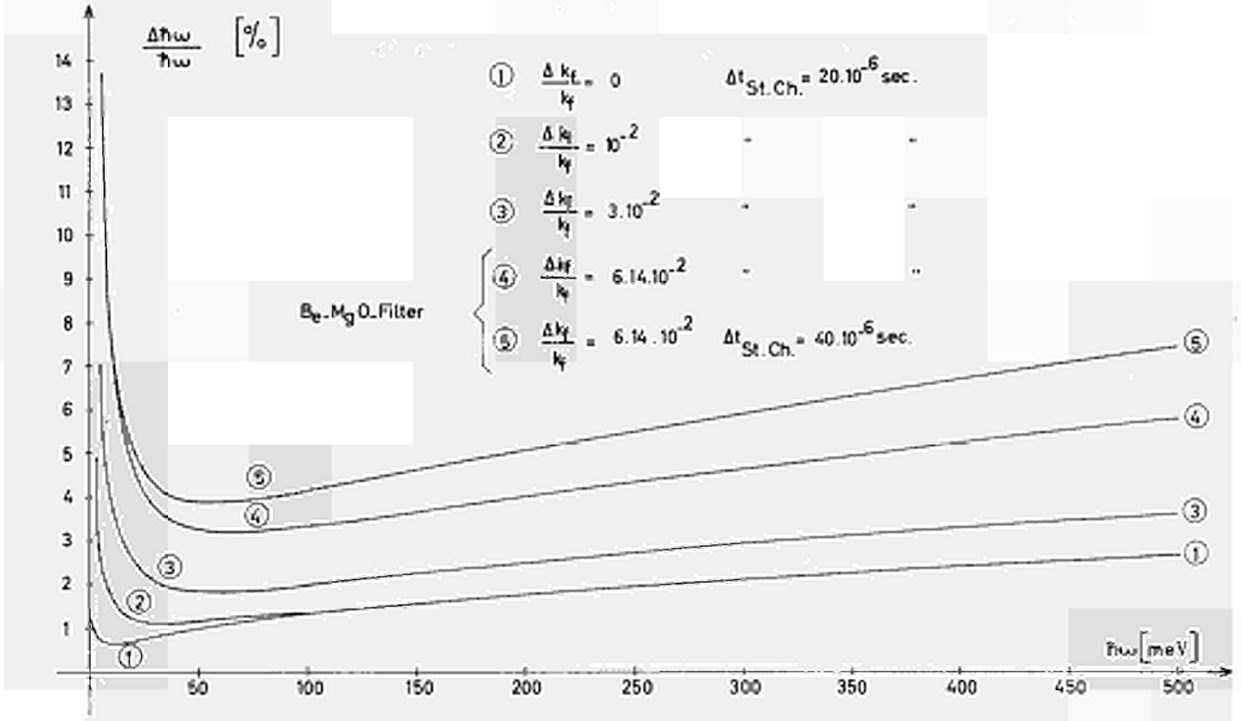

Fig. 11 THE RESOLUTION FUNCTION FOR THE INVERTED FACILITY FOR $k_f = 1{,}54\ Å^{-1}$ AND $l_f = 0{,}6$ m

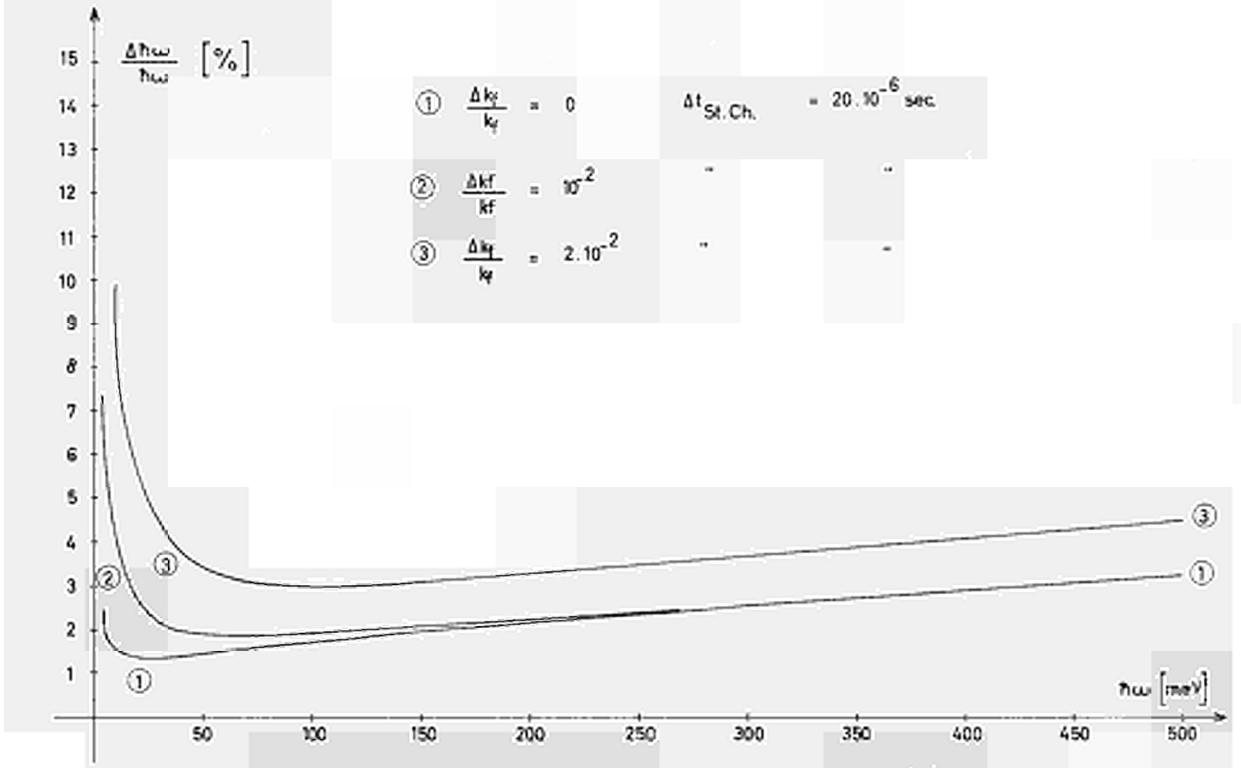

Fig. 12 THE RESOLUTION FUNCTION OF THE INVERTED FACILITY FOR $k_f = 2{,}5\ Å^{-1}$ AND $l_f = 2$ m

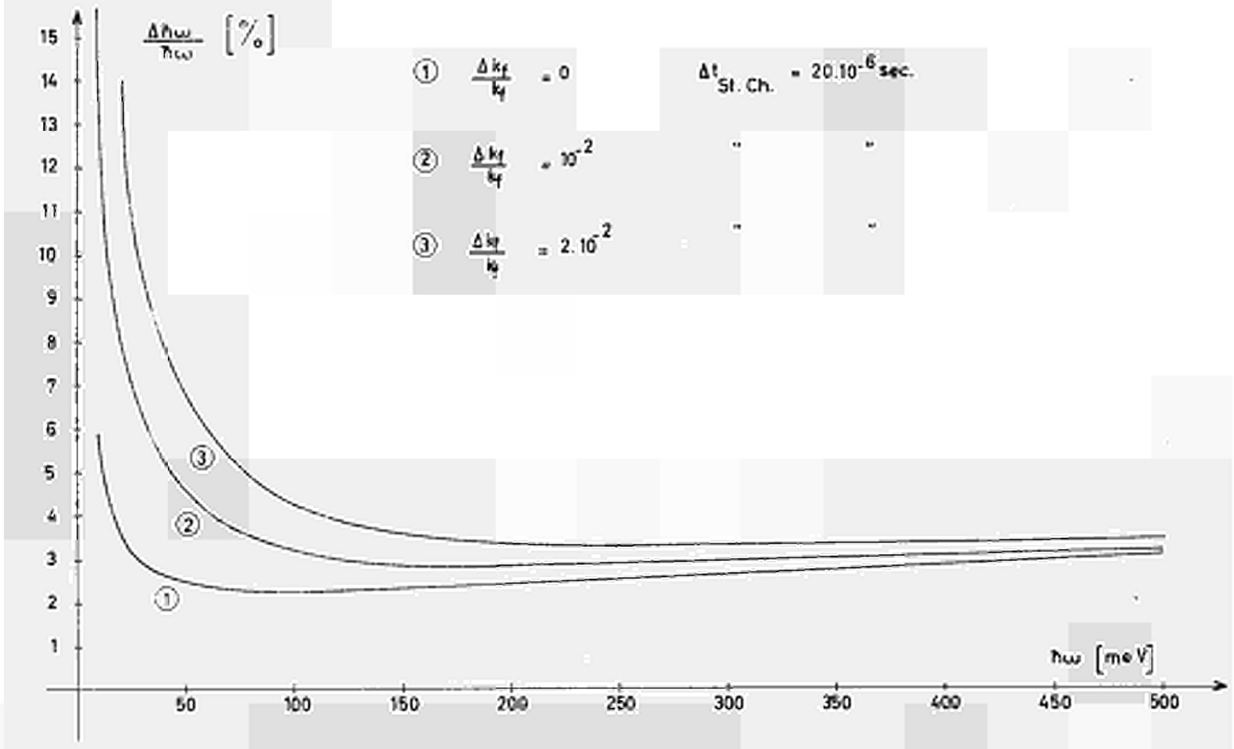

Fig. 13 THE RESOLUTION FUNCTION OF THE INVERTED FACILITY FOR $k_f = 5\,\text{Å}^{-1}$ AND $l_f = 2\,m$

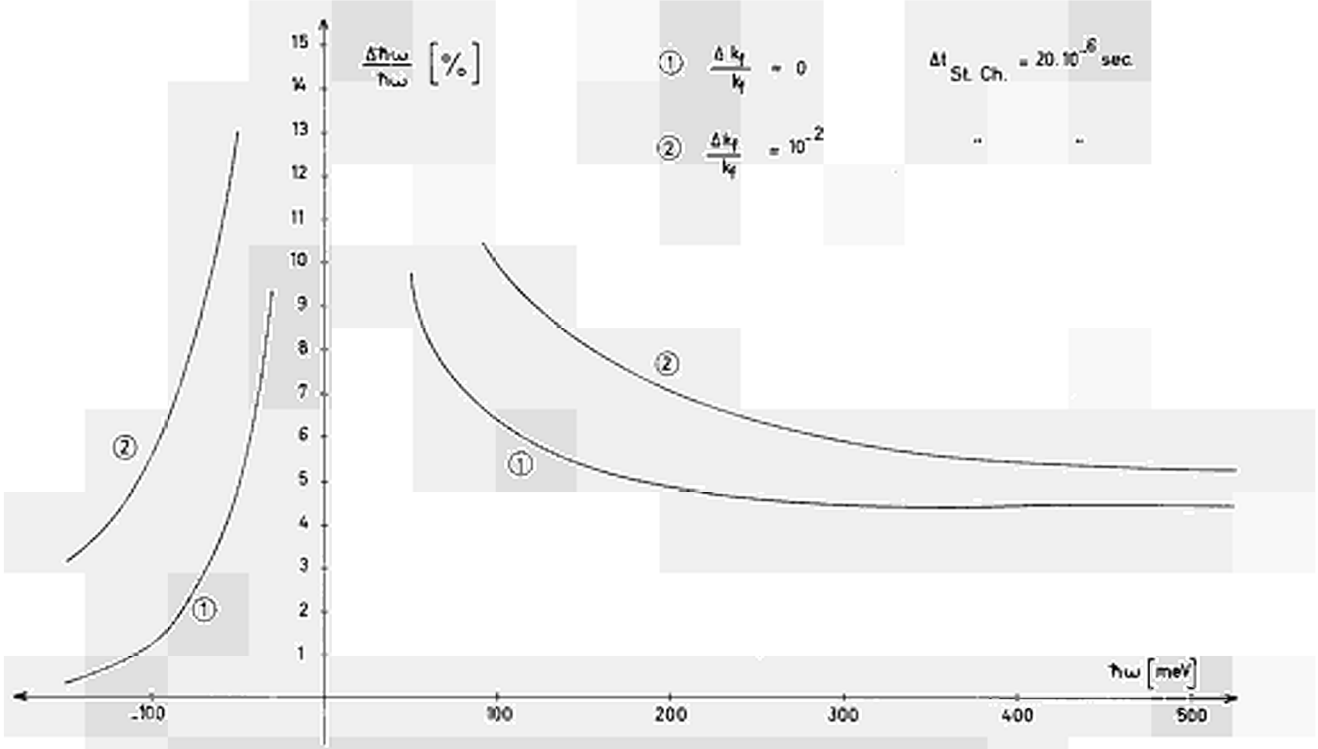

Fig. 14 THE RESOLUTION FUNCTION OF THE INVERTED FACILITY FOR $k_f = 10\,\text{Å}^{-1}$ AND $l_f = 2\,m$

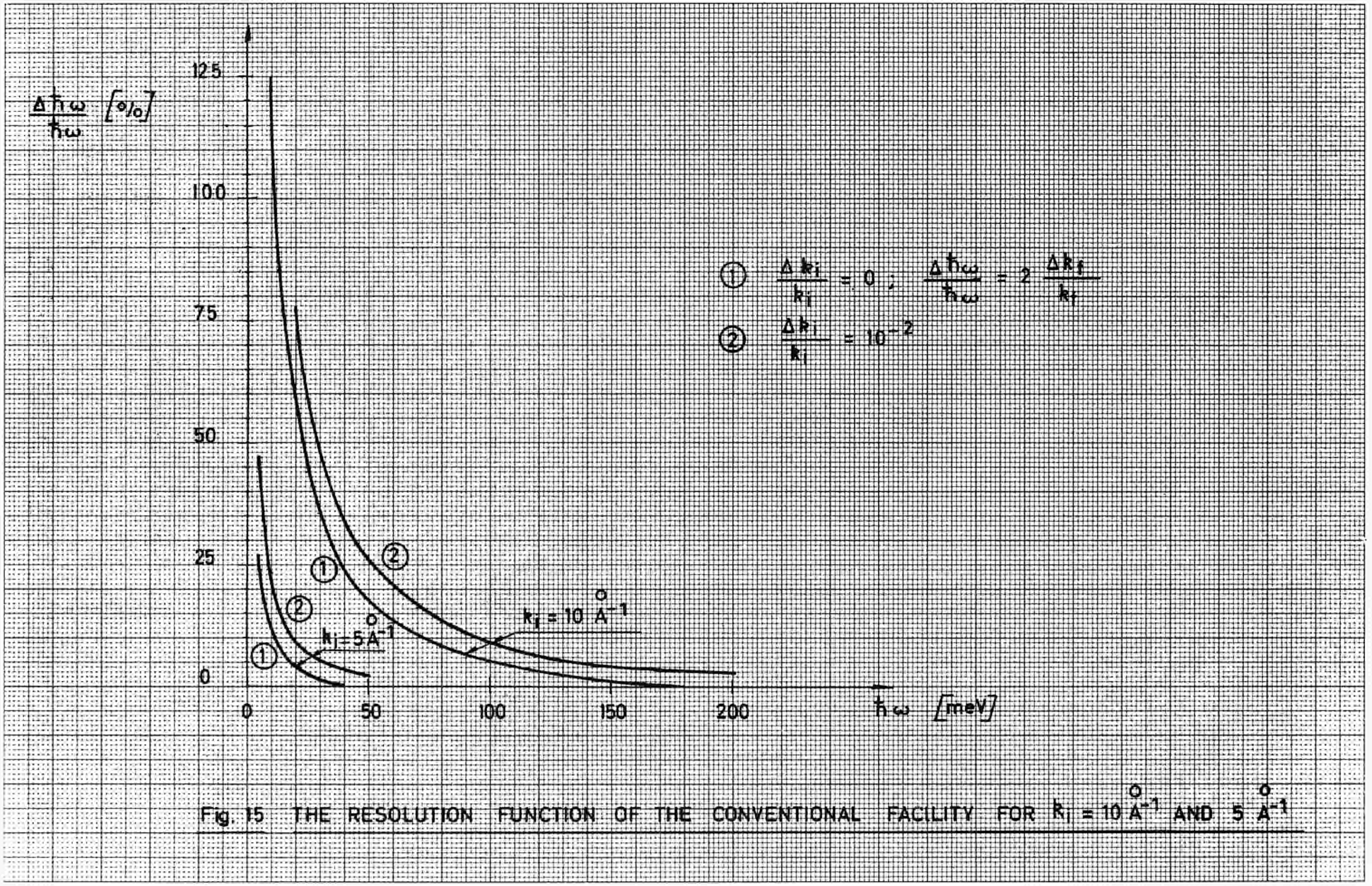

Fig. 15 THE RESOLUTION FUNCTION OF THE CONVENTIONAL FACILITY FOR $k_i = 10$ Å^{-1} AND 5 Å^{-1}

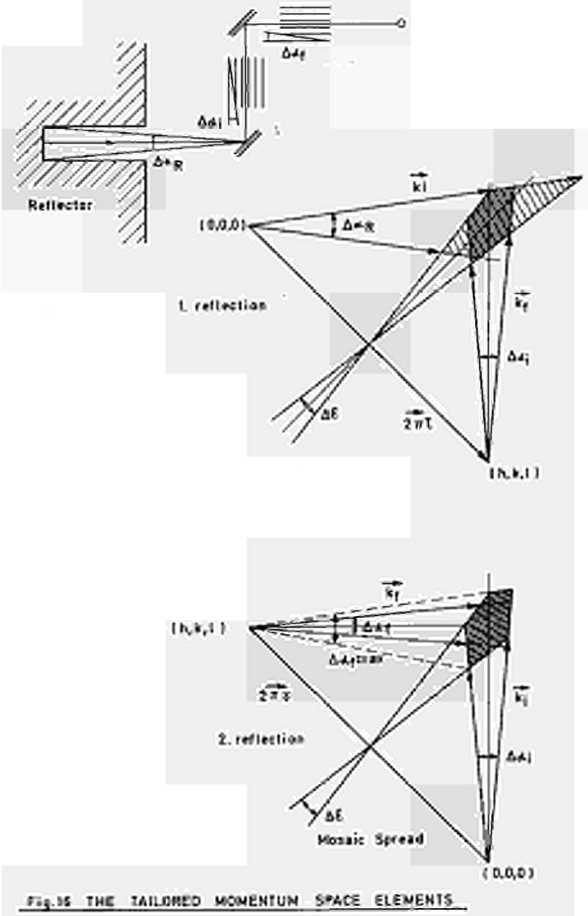

Fig. 16 THE TAILORED MOMENTUM SPACE ELEMENTS

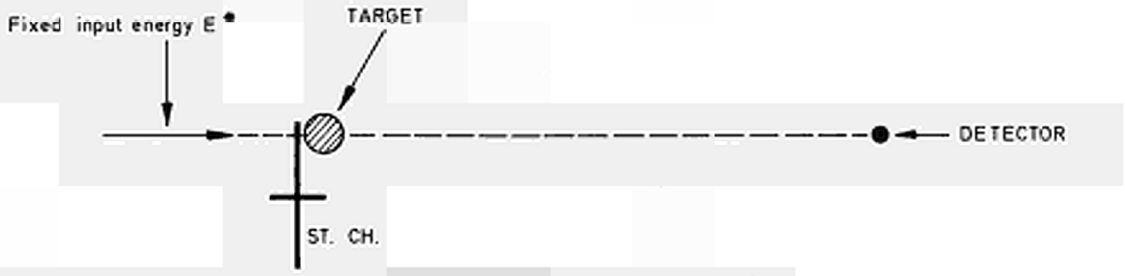

Fig. 17a : Normal (STATISTICAL) CHOPPER

Fig. 17 b : Inverted (STATISTICAL) CHOPPER

NOTICE TO THE READER

All scientific and technical reports published by the Commission of the European Communities are announced in the monthly periodical **"euro-abstracts".** For subscription (1 year: B.Fr. 1 025,—) or free specimen copies please write to:

Office for Official Publications
of the European Communities
Boîte postale 1003
Luxembourg 1
(Grand-Duchy of Luxembourg)

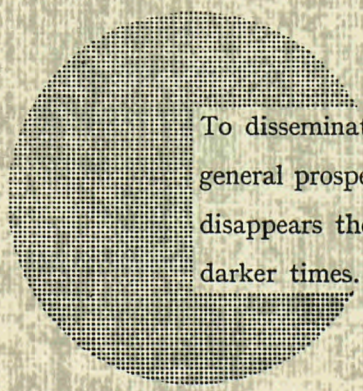

To disseminate knowledge is to disseminate prosperity — I mean general prosperity and not individual riches — and with prosperity disappears the greater part of the evil which is our heritage from darker times.

Alfred Nobel

SALES OFFICES

The Office for Official Publications sells all documents published by the Commission of the European Communities at the addresses listed below, at the price given on cover. When ordering, specify clearly the exact reference and the title of the document.

UNITED KINGDOM

H.M. Stationery Office
P.O. Box 569
London S.E. 1 — Tel. 01-928 69 77, ext. 365

BELGIUM

Moniteur belge — Belgisch Staatsblad
Rue de Louvain 40-42 — Leuvenseweg 40-42
1000 Bruxelles — 1000 Brussel — Tel. 12 00 26
CCP 50-80 — Postgiro 50-80

Agency :
Librairie européenne — Europese Boekhandel
Rue de la Loi 244 — Wetstraat 244
1040 Bruxelles — 1040 Brussel

DENMARK

J.H. Schultz — Boghandel
Møntergade 19
DK 1116 København K — Tel. 14 11 95

FRANCE

Service de vente en France des publications des Communautés européennes — Journal officiel
26, rue Desaix — 75 732 Paris - Cédex 15e
Tel. (1) 306 51 00 — CCP Paris 23-96

GERMANY (FR)

Verlag Bundesanzeiger
5 Köln 1 — Postfach 108 006
Tel. (0221) 21 03 48
Telex: Anzeiger Bonn 08 882 595
Postscheckkonto 834 00 Köln

GRAND DUCHY OF LUXEMBOURG

Office for Official Publications of the European Communities
Boîte postale 1003 — Luxembourg 6171
Tel. 4 79 41 — CCP 191-90
Compte courant bancaire: BIL 8-109/6003/200

IRELAND

Stationery Office — The Controller
Beggar's Bush
Dublin 4 — Tel. 6 54 01

ITALY

Libreria dello Stato
Piazza G. Verdi 10
00198 Roma — Tel. (6) 85 08
CCP 1/2640

NETHERLANDS

Staatsdrukkerij- en uitgeverijbedrijf
Christoffel Plantijnstraat
's-Gravenhage — Tel. (070) 81 45 11
Postgiro 42 53 00

UNITED STATES OF AMERICA

European Community Information Service
2100 M Street, N.W.
Suite 707
Washington, D.C., 20 037 — Tel. 296 51 31

SWITZERLAND

Librairie Payot
6, rue Grenus
1211 Genève — Tel. 31 89 50
CCP 12-236 Genève

SWEDEN

Librairie C.E. Fritze
2, Fredsgatan
Stockholm 16
Post Giro 193, Bank Giro 73/4015

SPAIN

Libreria Mundi-Prensa
Castello 37
Madrid 1 — Tel. 275 51 31

OTHER COUNTRIES

Office for Official Publications of the European Communities
Boîte postale 1003 — Luxembourg 6171
Tel. 4 79 41 — CCP 191-90
Compte courant bancaire: BIL 8-109/6003/200

OFFICE FOR OFFICIAL PUBLICATIONS OF THE EUROPEAN COMMUNITIES
Boîte postale 1003 — Luxembourg 6294

CDNA05047ENC